EDN: ZAGUGJ
УДК 621.373.826

Microstructural and Phase Transformations in Aluminium-Lithium Alloys after Laser Welding

Aleksander G. Malikov,* **Igor E. Vitoshki** ¶
Khristianovich Institute of Theoretical and Applied Mechanics SB RAS
Novosibirsk, Russian Federation
Evgeny V. Karpov §
Khristianovich Institute of Theoretical and Applied Mechanics SB RAS
Lavrentyev Institute of Hydrodynamics SB RAS
Novosibirsk, Russian Federation
Konstantin E. Kuper†
Khristianovich Institute of Theoretical and Applied Mechanics SB RAS
Budker Institute of Nuclear Physics of SB RAS
Novosibirsk, Russian Federation
Mariya I. Mironova ‡
Khristianovich Institute of Theoretical and Applied Mechanics SB RAS
Novosibirsk State University
Novosibirsk, Russian Federation
Alexey P. Zavialov ‖
Khristianovich Institute of Theoretical and Applied Mechanics SB RAS
Budker Institute of Nuclear Physics of SB RAS
Institute of Solid State Chemistry and Mechanochemistry SB RAS
Novosibirsk, Russian Federation

Received 03.10.2023, received in revised form 03.11.2023, accepted 04.12.2023

Abstract. The article shows the results of research on microstructural and phase transformation in aluminium-lithium alloys caused by laser welding followed by heat processing based on quenching and artificial aging. The microstructure and phase composition were examined with the help of synchrotron X-ray diffraction analysis and high-resolution electron microscopy. Two heat hardenable aluminium-lithium alloys used in the study are V-1461 and V-1469. The chosen alloys are notable for their high corrosion resistance, fracture and fatigue strength. V-1461 and V-1469 are third-generation alloys developed in FSUE "VIAM" and covered by Russian Federation Patents. The research shows that the structural-phase composition of alloys changes in the result of laser welding.

Keywords: laser welding, aluminum-lithium alloy, scanning electron microscopy, synchrotron radiation, x-ray diffractometry, mechanical properties.

Citation: A.G.Malikov, I.E.Vitoshkin, E.V.Karpov, K.E.Kuper, M.I.Mironova, A.P.Zavialov, Microstructural and Phase Transformations in Aluminium-Lithium Alloys after Laser Welding, J. Sib. Fed. Univ. Math. Phys., 2024, 17(1), 126–135. EDN: ZAGUGJ.

*smalik707@yandex.ru, ¶ igor.vitoshkin.97@mail.ru § evkarpov@mail.ru
†K.E.Kuper@inp.nsk.su, ‡ m.mironova@g.nsu.ru, ‖ zav_alexey@list.ru

Introduction

As of now, one of the principal objectives of aerospace engineering is to improve the weighting efficiency of the final product. Today, among the most challenging tasks in cooperative development of both new materials and advanced joint technologies lies the reduction of weight. In the early 90's, scientists introduced a number of third-generation Al–Li alloys with a reduced concentration of Li (Li $<$ 2 mass.%) in the following alloying systems: Al–Cu–Li (V-1461, V-1469, 2195, 2196, 2198, etc.), Al–Cu–Mg–Li (1441) and Al–Mg–Li (1424) [1, 2]. The indicated alloys are noted for their high mechanical properties due to special heat treatment, which, as a result, forms a number of strengthening phases: $\delta'(Al_3Li)$, $T_1(Al_2CuLi)$, $\theta'(Al_2Cu)$ [1, 3].

One of the most significant problems of aerospace engineering manifests itself in the necessity to find a substitution for the technology of riveting of modern aluminium alloys in the production of complex parts with unique performance properties that are constantly exposed to high thermal and mechanical stress through the use of new highly-efficient material-saving technologies that provide the target mechanical properties. Experts from All-Russian Scientific Research Institute of Aviation Materials (FSUE "VIAM" SRC of the Russian Federation) have estimated that substitution of riveted joints with welded joints comprised of aluminium-lithium alloys could reduce the weight of an aircraft by up to 25%. Airbus SE describes it as a «soft revolution» in aerospace engineering. However, it is important to note that modern technologies in fusion welding made it possible to produce heat hardenable aluminium and lithium-aluminium alloys with mechanical characteristics resembling 60 or 80% to that of an initial alloy [4].

Laser-welding of aluminium alloys of the Al–Cu–Li system requires knowledge of transformations that take place in structural and phase composition of weld joints. Phase composition of melting zone in a weld joint is determined by concentration ratio of alloying elements Cu, Li, Mg. in an initial alloy and by the filling material. Furthermore, the arrangement of strengthening phases in a solid solution and on the edge of dendrite in a weld joint can differ and not resemble that of the initial alloy. It is worth noting that it is rather difficult to determine a precise composition of a weld joint. To this day, precise methods of structural and phase composition management in weld joints are yet to be developed.

In this study, the phase composition was established with the help of synchrotron X-ray diffraction analysis. It is worth noting that synchrotron radiation has a number of primary benefits. For instance, it provides hard X-ray, its beam brightness in photons per second is 10^6 times higher than that of an X-ray tube, it can detect Li-rich phases with a size of less than 50 nm and phase composition in the volume of material, has a small beam area (100×400 μm), which makes it possible to carry out a local analysis of the material volume. Moreover, synchrotron does not require complicated specimen preparation.

The aim of this paper is to study the structural and phase transformation of aluminium alloys caused by laser welding followed by heat processing based on quenching and artificial aging with the use of synchrotron radiation and high-resolution electron microscopy.

1. Experimental procedure

In the present study laser welding of a 1.5 mm Al–Cu–Li system aluminium-lithium alloy was carried out with the help of a CO_2 laser with maximum power output of 8 kW. The above mentioned laser is a part of ALTC "Sibir" developed at the ITAM SB RAS (Russia).

Two aluminium-lithium alloys were used in the research, namely V-1469 of the Al-3.9Cu-0.3Mg-1.2Li system and V-1461 of the Al-2.7Cu-0.3Mg-1.8Li system developed at FSUE

"VIAM" [5]. These alloys come in the form of α-Al solid solution with phase-creating alloying elements applied on aluminium. Tab. 1 represents a number of principal strengthening phases [5, 6]. Notation used is as follows: ρ is density, λ is thermal conductivity, C_p is heat capacity, σ_{uts} is ultimate tensile strength, σ_y is yield strength, δ is elongation at break.

Table 1. Physical and mechanical properties of aluminium-lithium alloys

Alloy	Principal strengthening phases	ρ, g/cm^3	λ, W/(m·K)	C_p, J/kg·K	σ_{uts}, MPa	σ_y, MPa	δ, %
V-1461	$\delta'(Al_3Li)$, T_1 (Al_2CuLi)	2.64	92	910	550	470	10.1
V-1469	$\theta'(Al_2Cu)$, T_1 (Al_2CuLi)	2.69	86	930	556	514	10.4

Fig. 1 represents a scheme used over the course of metallographic analysis with the help of optical and scanning electron microscopy along with the structural-phase analysis carried out using synchrotron radiation on a megascience class facility.

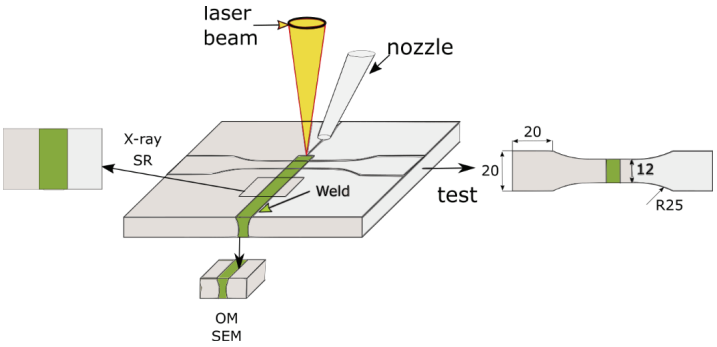

Fig. 1. Scheme of welding and specimen preparation for metallographic analysis

Specimen preparation process is described in detail in [7]. Post heat treatment process was optimized. Quenching was conducted in water following a 30 minutes' heating in a muffle furnace under 500 °C to 560 °C temperatures. Heating rate equaled 5 °C/min. Artificial aging was completed in 12 to 32 hours' time under temperatures of 140 °C to 200 °C. Heating rate is 5 °C/min.

2. Experimental results

An optimization process was carried out for energy parameters of laser welding, such as welding speed, radiation rate, diameter, depth and location of the focal area.

Visual defects imply cracks, lack of penetration, discontinuity flaws, undercuts, cavities, insufficiencies and open porosity of weld joints. The quality factors of the internal microstructure and morphology of a laser weld joint are minimum porosity, equal width of both its upper and root parts and also its capability of forming an X-shaped vertical joints with two curvilinear bevels [8].

Laser beam power range W was 2–3.5 kW, focal area of laser beam ranged from –3 to +3 mm of the surface, welding speed V was 2–5 m/min (33.3–100 mm/s), nozzle gas consumption — from 3 to 15 l/min. Laser beam was focused with the help of a ZnSe lens with a focal distance of $f = 254$ mm.

Tab. 2 suggests optimal conditions under which it is possible to produce laser welded joints with no visual defects such as undercuts, discontinuity flaws, cracks, pores and sagging. W indicates laser beam power, V is welding speed, t is alloy thickness, h is average width of the weld joint. The table also represents the energy requirements needed to produce a high-quality weld joint under optimal conditions for the suggested plate thickness. Heat input $P = W/V$, energy to weld joint height $P_{\text{depth}} = W/V$, $E_{\text{depth}} = W/tV$ is energy to linear surface, $E = W/V_{\text{th}}$ is energy to one volumetric unit of melted material, in which W denotes power, V is welding speed, t is alloy thickness, h is average width of a weld joint.

Table 2. Optimal conditions for laser welding

Alloy	t, mm	W, kW	V, m/min	Δf, mm	P, J/mm	P_{depth}, J/s·mm	E_{depth}, J/mm^2	E, J/mm^3
V-1461	2	3.3	4	-3	49.5	1650	24.75	25.25
V-1469	1.8	3.5	4	-3	52	1944	29.17	22.27

Fig. 2 represents the general view of the cross section of the weld joints, microstructure of the weld junction of the fusion zone (FZ) and of the heat affected zone (HAZ). Images were taken with the help of an optical microscope.

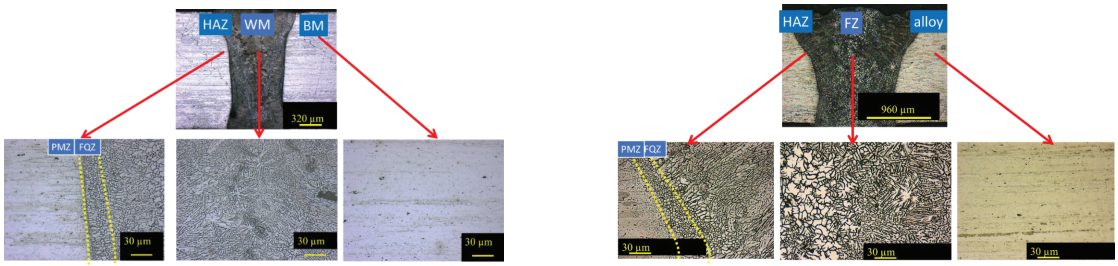

(a) (b)

Fig. 2. Microstructure of the cross section of the welded joint and the alloy. General view: (a) — V-1461 of the Al-2.7Cu-0.3Mg-1.8Li system, (b) – V-1469 of the Al-3.9Cu-0.3Mg-1.2Li system

As shown in Fig. 2, an equiaxial dendrites grains can be observed in the fusion zone. Heat affected zone consists of rod-like dendrites, while Zr- and Li-rich aluminium alloys, in addition to rod-like dendrites, have an equiaxed zone of spherical dendrites. Today, heterogeneous nucleation that comes out of $\beta'(Al_3Zr)$ and $Al_3(Lix,Zr1\text{-}x)$ phases present in the initial alloy is generally accepted as a building mechanism of the equiaxed zone [9]. The $\beta'(Al_3Zr)$ equilibrium phase provides a proper and efficient center for heterogeneous nucleation during crystallization.

It is of note that during the process of laser welding crystallization structure is largely determined by heat conditions and temperature changes. As for microstructure, it is determined by two key parameters: temperature gradient G and crystallization rate R. When it comes to dendrite structure, it is regulated by G/R relation, and, since laser welding provides a high crystallization rate R, the structure of weld joints in aluminium alloys is comprised of dendrite grains. Thus, relation of thermal influence (cooling rate) with present parameters is $dT/dt = GR$.

Therefore, G/R relation forms the morphology of the resulting grain structure, while an increase in cooling rate leads to intensification in nucleation, in other words, to grain refinement. Hence, $G{\cdot}R$ determines the grain size. According to the literature [10], the equation for the

temperature gradient on the isotherm liquidus line becomes as follows:

$$G/R = 2\pi \frac{(T_{\text{liq}} - T_0)^3}{\eta_{\text{abs}}^2 * P_{\text{depth}}^2} \lambda V \rho C_p \,. \tag{1}$$

The equation for the cooling rate becomes:

$$\frac{dT}{dt} = GR = 2\pi \frac{(T_{\text{liq}} - T_0)^3}{\eta_{\text{abs}}^2 * E_{\text{depth}}^2} \lambda \rho C_p, \tag{2}$$

where T_{liq} is liquidus temperature, η_{abs} is radiation absorption coefficient. $T_{\text{liq}} = 650$ °C, $\eta_{\text{abs}} = 0.8$. Target values of G/R and dT/dt are listed in Tab. 3.

Table 3. Target values of G/R and dT/dt

Alloy	dT/dt	G/R
V-1461	2570	0.58
V-1469	1805	0.4

Fig. 3 shows the fusion zones of alloys under study at 4000^x and $100\,000^x$ zoom SEM analysis.

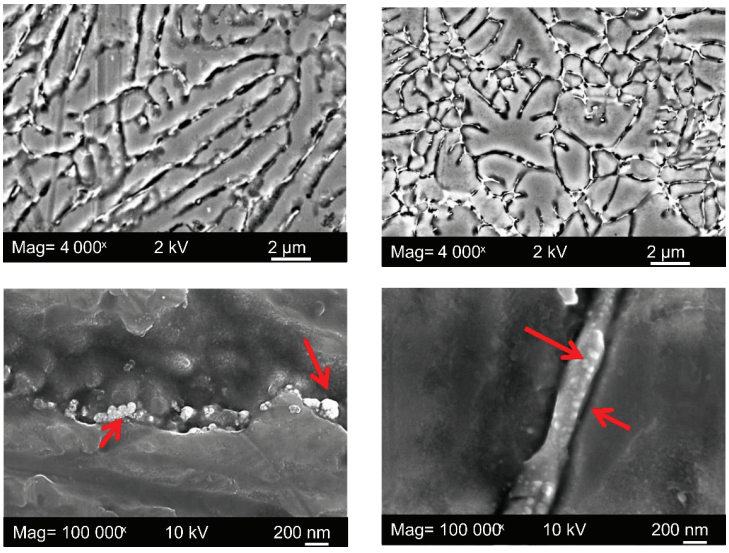

(a) (b)

Fig. 3. SEM analysis of micro- and nanostructures of the weld joint: (a) B-1461 alloy, (b) B-1469 alloy. 4000^x and $100\,000^x$ zoom

As it is seen in Fig. 3, dendrite structure has been formed during crystallization in the result of laser welding. Agglomerate particles of various phases are mainly located on the edges of dendrite grains. Specifically, a number of small 60–150 nm bright particles can be observed on the edges of dendrites.

Fig. 4 shows X-ray patterns of the initial alloy, heat affected zone (HAZ) and fusion zone of the laser welded joint. The results were obtained with the help of synchrotron X-ray diffraction analysis.

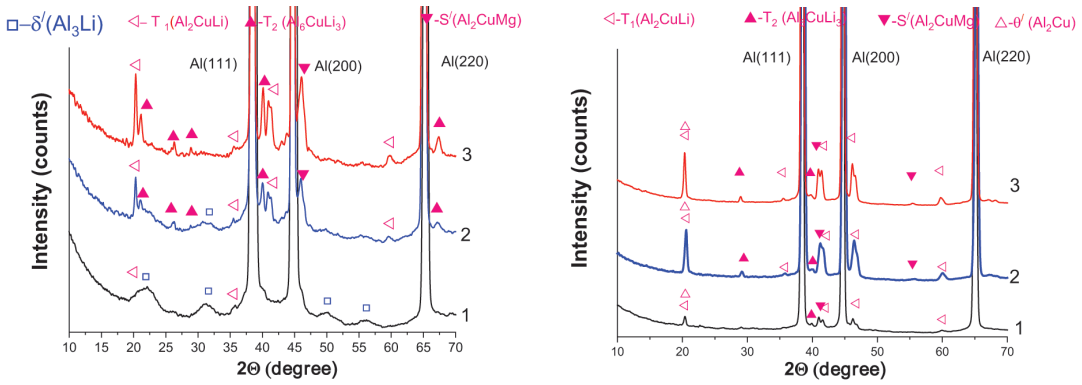

(a) (b)

Fig. 4. X-ray patterns of the welded joint specimens: (a) V-1461 alloy, (b) V-1469 alloy. 1 — alloy, 2 — HAZ, 3 — FZ

According to the results of synchrotron analysis and high-resolution microscopy (Figs. 3 and 4), it is safe to assume that $T_1(Al_2CuLi)$ and $T_2(Al_6CuLi_3)$ phases form on the dendrite boundary of V-1461 alloy. As for V-1469 alloy, which is relatively Cu-rich, the formation of $T_1(Al_2CuLi)$ and $\theta(Al_2Cu)$ phases can be observed. The role of the above mentioned phases in the process of strengthening depends on the concentration of the alloying elements Cu, Li and Mg. It is worth noting that the mechanical properties of the welded joint specimens become relatively low (Tab. 4).

Table 4. Mechanical properties of the welded joint specimens

Alloy	Welded joint specimen					
	σ_{uts}, MPa	σ_{ys},	δ, %	k_1,%	k_2,%	k_3,%
V-1461	341	333	0.7	62	71	7
V-1469	310	295	0.7	55	57	6

In this table k_1 denotes ultimate tensile strength, k_2 — yield strength, k_3 — elongation at break as compared to the properties of the initial alloy.

Now, the mechanical properties are relatively low due to a rapid change of structural-phase composition of the welded joints that occur as the result of heating, melting and crystallization.

To improve the mechanical properties, such post heat treatment methods as quenching and artificial aging have been used.

Fig. 5 shows typical relations of the average σ_{uts}, σ_{ys} and δ of the weld joint specimen in relation to quenching temperatures.

According to Fig. 5, optimal quenching temperatures that provide maximum ultimate tensile strength for V-1461 and V-1469 are 530 °C and 560 °C respectively. After quenching, the samples were subjected to artificial aging under various temperature-time conditions.

Fig. 6 shows specific changes of the ultimate tensile strength in relation to temperature-time conditions received by means of test value approximation using the least squares method. For the sake of convenience, the colored ultimate tensile strength Z scale is depicted on the right.

It has been discovered that weld joints of the V-1461 alloy of the Al-2.7Cu-0.3Mg-1.8Li system match the mechanical properties of the initial alloy after the following procedure: 530 °C

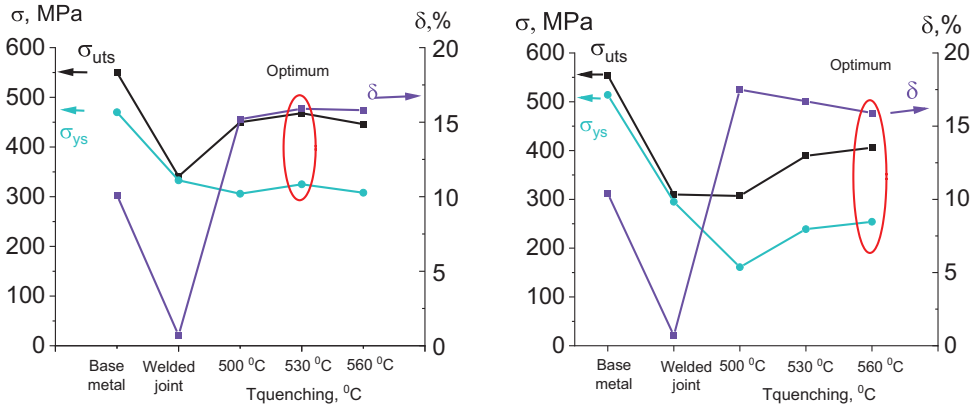

Fig. 5. Mechanical properties σ_{uts}, σ_{ys}, and δ of the weld joint specimen in relation to quenching temperatures: (a) V-1461 alloy, (b) V-1469 alloy

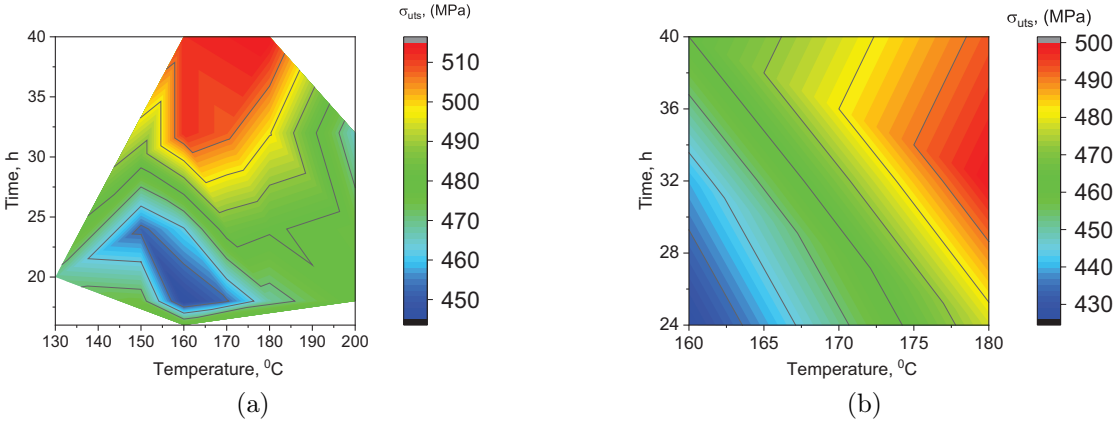

Fig. 6. Ultimate tensile strength σ_{uts} in relation to temperature-time condition, (a) V-1461 alloy, (b) V-1469 alloy

quenching with 30 min aging followed by the process of artificial aging under 170 °C temperature with an additional 32-hour aging.

As for the weld joints of the V-1469 alloy of an Al-3.9Cu-0.3Mg-1.2Li system, the procedure becomes as follows: 530°C quenching with 30 min aging followed by the process of artificial aging under 180 °C temperature with an additional 32-hour aging.

Fig. 7 shows X-ray patterns of the initial alloy and the fusion zone of the welded joint before and after HT. The results were obtained with the help of synchrotron X-ray diffraction analysis.

According to Fig. 7, phase state of the weld joint after optimal heat treatment becomes somewhat similar to that of the initial alloy.

When concentration of Cu is relatively low ($C^{Cu}/C^{Li} = 1.5$, as in V-1461 alloy), the weld joint has a $T_1(Al_2CuLi)$ phase and a slight amount of a $T_2(Al_6CuLi_3)$ phase. However, after quenching, as $T_1(Al_2CuLi)$ and $T_2(Al_6CuLi_3)$ phases dissolve, a $\delta'(Al_3Li)$ phase is formed.

As concentration of Cu in V-1469 rises ($C^{Cu}/C^{Li} = 3.25$), both in the alloy and in the weld joint without HT, a $T_1(Al_2CuLi)$ and a $\theta(Al_2Cu)$ phase can be observed. Due to these lithium particles we can observe a 127 MPa increase of the weld joint strength in the V-1461 alloy.

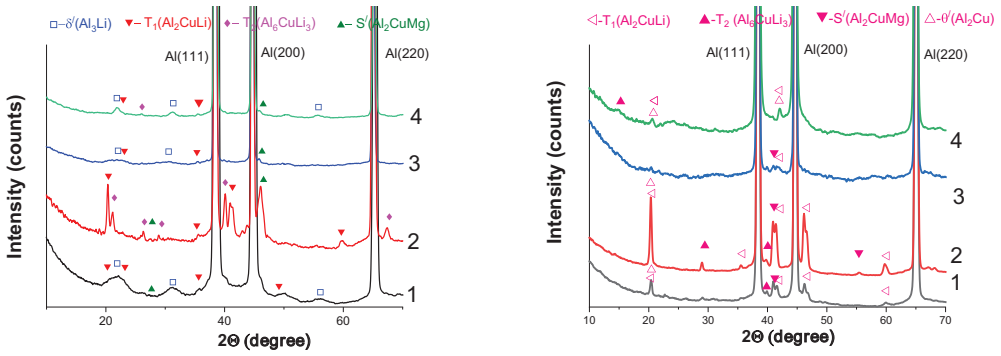

(a) (b)

Fig. 7. X-ray patterns of the weld joint specimens: (a) V-1461 alloy, (b) V-1469 alloy. 1 — alloy, 2 — weld joint, 3 — weld joint after quenching, 4 — weld joint after quenching and artificial aging

Fig. 8 shows changes in ultimate tensile strength $\Delta\sigma_{\text{uts}}$, yield strength $\Delta\sigma_{\text{ys}}$ and elongation $\Delta\delta$ of the weld joint in accordance with its phase composition after optimal quenching.

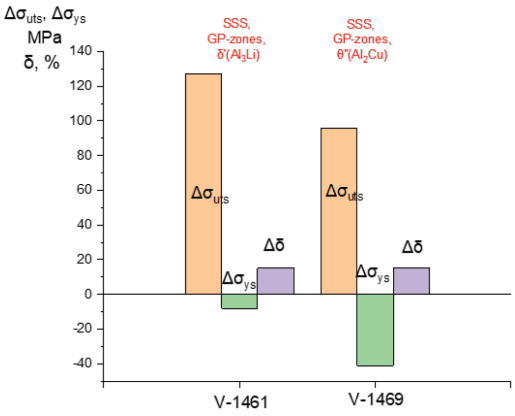

Fig. 8. Changes in structural-phase composition of the weld joints after optimal quenching. (SSS — Supersaturated Solid Solution, GP-zones — Guinier–Preston zones)

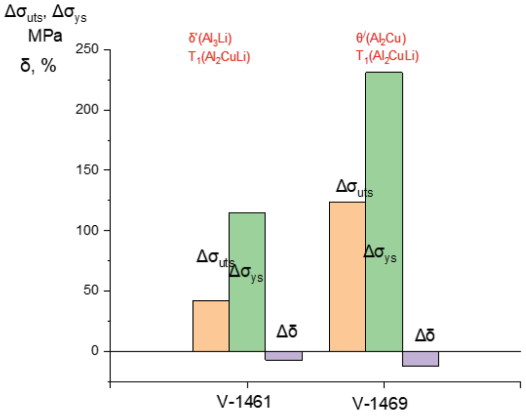

Fig. 9. Changes in structural-phase composition of the weld joints after optimal artifial aging

Fig. 9 demonstrates changes in ultimate tensile strength $\Delta\sigma_{\text{uts}}$, yield strength $\Delta\sigma_{\text{ys}}$ and elongation $\Delta\delta$ of the weld joint in accordance with its phase composition after optimal artifial aging.

Therefore, the conducted research makes it possible to determine the phase transformation chains for the alloys under analysis.

For the Al–Cu-Mg-Li system they are as follows:

For Cu/Li $>$ 3; SSS $\rightarrow$ GP-zones $\rightarrow\theta''\rightarrow\theta'$ 1

For Cu/Li $=$ 1 – 2.5; SSS $\rightarrow$ GP-zones $+\delta'\rightarrow\theta'+\delta'\rightarrow\delta'+\mathrm{T_1}\rightarrow\mathrm{T_1}$ 2

For Cu/Li $<$ 1; SSS $\rightarrow$ GP-zones $+\delta'\rightarrow\delta'+\mathrm{S'}$ 3

It is of note that GP-zones, coherent and semi-coherent phases cannot be experimentally observed. However, thanks to synchrotron radiation, final phase composition after melting, quenching and artificial aging can be successfully detected with the help of synchrotron radiation.

Tab. 5 lists the mechanical properties of the weld joints and their relation to the initial alloy: k_1 is ultimate tensile strength, k_2 is yield strength, k_3 is elongation at break in relation to the properties of the initial alloy after optimal heat treatment.

Table 5. Mechanical properties of welded joints of aluminium-lithium alloys obtained in static tensile tests

Alloy	Welded joint sample					
	σ_{uts}, MPa	σ_{ys}, MPa	δ, %	k_1,%	k_2,%	k_3,%
V-1461	510	440	8.7	93	94	86
V-1469	530	485	3.9	95	94	38

Mechanical strength properties obtained under optimal laser welding conditions become close or equal to that of the initial alloys as received.

Conclusions

An analysis of the structural-phase composition of welded joints of aluminium-lithium third-generation V-1461 and V-1469 alloys was successfully carried out with the help of synchrotron radiation and scanning electron microscopy.

Evolution of the phase composition of V-1461 of the Al-2.7Cu-0.3Mg-1.8Li system is as follows: the welded joint ($\acute{\alpha}$ Al+ $T_1(Al_2CuLi)$ + $T_2(Al_6CuLi3)$) ▶ quenching ($\acute{\alpha}$ Al + supersaturated solid solution ▶ G-P zones ▶ $\delta'(Al_3Li)$ ▶ artificial aging ($\acute{\alpha}$+ $\delta'(Al_3Li)$ + $T_1(Al_2CuLi)$).

Evolution of the phase composition of V-1469 of the Al-3.9Cu-0.3Mg-1.2Li system is as follows: the welded joint ($\acute{\alpha}$ Al+ $T_1(Al_2CuLi)$) ▶ quenching (α Al + supersaturated solid solution ▶ G-P zones ▶ $\theta''(Al_2Cu)$ ▶ artificial aging ($\acute{\alpha}$ + $\theta'(Al_2Cu)$ + $T_1(Al_2CuLi)$).

This research was funded by the Russian Science Foundation, grant number 23-79-00037 (https://rscf.ru/project/23-79-00037/).

Part of the work was done at the shared research center SSTRC on the basis of the VEPP-4 - VEPP-2000 complex at BINP SB RAS.

References

[1] A.Abd El-Aty, Y.Xu, X.Guo, S.-H.Zhang, Y.Ma, D.Chen, *J. Adv. Res.*, **10**(2018), 49.

[2] T.Dorin, A.Vahid, J.Lamb, Fundam. Alum. Metall., Elsevier, 2018, 387–438. DOI: 10.1016/B978-0-08-102063-0.00011-4

[3] T. Dursun, C. Soutis, *Mater. Des.*,**56**(2014), 862.

[4] N.Kashaev, V.Ventzke, G.Çam, *J. Manuf. Process.*, **36**(2018), 571. DOI: 10.1016/j.jmapro.2018.10.005

[5] E.N.Kablov, V.V.Antipov, J.S.Oglodkova, M.S.Oglodkov, *Metallurgist*, **65**(2021), 72. DOI: 10.1007/s11015-021-01134-9

[6] N.I.Kolobnev, L.B.Khokhlatova, E.A.Lukina, Trends in the development of aluminum-lithium alloys and technology of their processing, Moscow, All-Russian Research Institute of Aviation Materials, 2019.

[7] A.G.Malikov, A.M.Orishich, *Int. J. Adv. Manuf. Technol.*, **94**(2018), 2217–2227. DOI: 10.1007/S00170-017-0860-6

[8] S.Katayama, Handb. Laser Weld. Technol. Elsevier, 2013, 332–373.

[9] Y.N.Hu, S.C.Wu, L.Chen, *Eng. Fract. Mech.*, **208**(2019), 45.

[10] C.Hagenlocher, F.Fetzer, D.Weller, R.Weber, T.Graf, *Mater. Des.*, **174**(2019), 107791. DOI: 10.1016/j.matdes.2019.107791

Исследование структурных и фазовых превращений в алюминиево-литиевых сплавах при высокоэнергетическом лазерном воздействии

А.Г. Маликов
И.Е. Витошкин
Институт теоретической и прикладной механики им. С. А. Христиановича СО РАН
Новосибирск, Российская Федерация
К.Э. Купер
Институт теоретической и прикладной механики им. С. А. Христиановича СО РАН
Институт ядерной физики им. Г. И. Будкера СО РАН
Новосибирск, Российская Федерация
Е.В. Карпов
Институт теоретической и прикладной механики им. С. А. Христиановича СО РАН
Институт гидродинамики им. М. А. Лаврентьева СО РАН
Новосибирск, Российская Федерация
М.И. Миронова
Институт теоретической и прикладной механики им. С. А. Христиановича СО РАН
Новосибирский национальный исследовательский государственный университет
Новосибирск, Российская Федерация
А.П. Завьялов
Институт теоретической и прикладной механики им. С. А. Христиановича СО РАН
Институт ядерной физики им. Г. И. Будкера СО РАН
Институт химии твёрдого тела и механохимии СО РАН
Новосибирск, Российская Федерация

Аннотация. В данной работе приведены результаты исследований структурных и фазовых превращений в алюминий-литиевых сплавах при высокоэнергетическом лазерном воздействии и последующей термообработке на основе процесса закалки и искусственного старения. Структура и фазовый состав были исследованы с использованием синхротронного излучения и высокоразрешающей электронной микроскопии. В качестве термически упрочняемых алюминий-литиевых сплавов были выбраны следующие марки: сплав В-1461 и сплав В-1469. Эти сплавы обладают высокой коррозионной стойкостью, трещиностойкостью и усталостной долговечностью. Сплавы марки В-1461 и В-1469 являются сплавами 3-го поколения, они разработаны в ФГУП «ВИАМ» и защищены патентами РФ. Было показано, что в процессе сварки происходит изменение структурно-фазового состава. В твердом растворе сварного шва упрочняющие фазы растворяются, а фазы различного типа для медесодержащих сплавов формируются на границе дендрита. Пост–термообработка лазерных сварных соединений в виде процесса закалки и искусственного старения позволяет восстанавливать структурно-фазовый состав сварного шва и повысить механические характеристики до уровня исходного сплава.

Ключевые слова: лазерная сварка, алюминиево-литиевый сплав, растровая электронная микроскопия, синхротронное излучение, рентгеновская дифрактометрия, механические свойства.